



## The Effect of Emission Control on the Submicron Particulate Matter Size Distribution in Hangzhou during the 2016 G20 Summit

Huan Yu<sup>1\*</sup>, Wei Dai<sup>1</sup>, Lili Ren<sup>1</sup>, Dan Liu<sup>1</sup>, Xintian Yan<sup>1</sup>, Hang Xiao<sup>2</sup>, Jun He<sup>3</sup>, Honghui Xu<sup>4</sup>

<sup>1</sup> School of Environmental Science and Engineering, Nanjing University of Information Science and Technology, Nanjing 210044, China

<sup>2</sup> Institute of Urban Environment, Chinese Academy of Sciences, Xiamen 361021, China

<sup>3</sup> Research Group of Natural Resources and Environment, International Doctoral Innovation Center, Department of Chemical and Environmental Engineering, University of Nottingham Ningbo China, Ningbo 315100, China

<sup>4</sup> Zhejiang Meteorological Science Institute, Hangzhou 310051, China

---

### ABSTRACT

A number of observational and modeling studies have been conducted in China to study the effectiveness of radical short-term emission control measures with regard to air quality improvement. However, none of them have focused on the effect on submicron aerosols. Measurements on the size distribution of particles as small as 3 nm were conducted before, during and after the source emission control period for the 2016 G20 Summit held in Hangzhou, a megacity in eastern China. The measurement provided a unique opportunity to gain insight into the sources of submicron aerosols in Hangzhou and the effectiveness of radical emission control strategies. A WRF-Chem simulation suggested that the sources inside the emission control region contributed more than 70% to PM<sub>1</sub> in Hangzhou from September 2 to 7, 2016, even under the strictest control scheme. Source restrictions on emissions from coal-fired power plants, on-road vehicles and industrial VOCs resulted in concentration decreases for PM<sub>1</sub>, PM<sub>0.01</sub> and PM<sub>0.1</sub>, respectively. New particle formation (NPF) events, which were not suppressed completely by the emission control, enhanced the maximum PM<sub>0.01</sub> concentration, at around 11:00 AM, by a factor of 4 compared to non-NPF days. Even during the strictest emission control period, two PM<sub>1</sub> episodes still occurred due to the dominance of subsidence airflows, a low wind speed, and a weak vertical temperature gradient.

**Keywords:** Urban aerosols; Submicron aerosols; Particle size distribution; Emission control strategy.

---

### INTRODUCTION

Size distribution is a key physical property of particulate matter (PM) in understanding its sources, atmospheric processes, health effect and radiative forcing (Pui *et al.*, 2014). Submicron PM, or particles with an aerodynamic diameter of up to 1 μm (PM<sub>1</sub>), have prompted a strong research interest in the scientific community due to their adverse health effect, complicated secondary formation pathways, strong light attenuation and long lifetime in the atmosphere (Sun *et al.*, 2011; IPCC, 2013; Gaston *et al.*, 2014; Singh and Gupta, 2016; Zhang *et al.*, 2017). Ultrafine PM, or particles with a diameter up to 100 nm (PM<sub>0.1</sub>), is even more toxic than PM<sub>1</sub> (Ostro *et al.*, 2015). Nevertheless, the chemical composition measurement and source apportionment of PM<sub>0.1</sub> is very difficult, due to their low

mass loading in the atmosphere. Sub-10 nm particle, or PM<sub>0.01</sub>, is a key concern of atmospheric new particle formation (NPF) study and combustion science (Shi *et al.*, 2001; Kim *et al.*, 2015; Kulmala *et al.*, 2017). These particles are believed to be emitted by combustion sources or formed in regional and local nucleation events and eventually grow to the “accumulation” mode via coagulation and surface condensation in the atmosphere (Guo *et al.*, 2014).

Submicron particles in megacities are of particular research interest due to their complex sources and the high population exposure level to the polluted urban atmosphere (Shen *et al.*, 2009; Carbone *et al.*, 2013; Aurela *et al.*, 2015). Chemical Mass Balance source apportionment studies in Hangzhou, a hub megacity in eastern China, showed that more than 70% of PM<sub>1</sub> in Hangzhou can be attributed to secondary particles (sulfate, nitrate and secondary OC) and vehicle emission (Shen *et al.*, 2014; Wu *et al.*, 2014). Regional CMAQ modeling by Hu *et al.* (2015) also showed that vehicle emission is the number one contributor to PM<sub>2.5</sub> in Hangzhou (34%). Based on these studies, it seems that vehicle emission control will be one of the most

---

\* Corresponding author.

E-mail address: hyu@nuist.edu.cn

effective strategies to reduce fine PM in Hangzhou, although there is also evidence that air mass cross-border transports led to high PM formation in Hangzhou in heavy haze episode (Yu *et al.*, 2014).

The “2016 G20 summit” was held on September 4–5, 2016, in Hangzhou. Local government enforced a temporary three-phase emission control scheme in Hangzhou and the surrounding regions within 100 km from Hangzhou on the basis of real-time air quality forecast and “Environmental Quality Guarantee Scheme for Zhejiang Province during the G20 2016 Hangzhou Summit” (Fig. S1, supporting information). The emission control scheme, as shown in Fig. 1, included a coal-fired power plant capacity 50% reduction from August 24 to September 6, followed by “odd-even” on-road vehicle restriction (not applicable to public service vehicles; an approximate 50% vehicle emission reduction was assumed in this paper) from August 28 to September 6 and 100% industrial VOC reduction from industrial sectors (e.g., refinery and chemical processes/facilities) from August 31 to September 6. The emission control provides a unique opportunity to investigate the possible sources of PM in Hangzhou.

A number of observation and modeling studies have been conducted in China to study the effectiveness of short-term emission control schemes on air quality improvement (Wang *et al.*, 2010; Huang *et al.*, 2013; Meng *et al.*, 2015; Hua *et al.*, 2016; Zhou *et al.*, 2016; Guo *et al.*, 2017; Li *et al.*, 2017; Wang *et al.*, 2017; Yang *et al.*, 2017). However, none of them have focused on the effect on submicron aerosols. In this study, particle size distribution down to 3 nm, water-soluble inorganic ions of submicron aerosols and peroxyacetyl nitrate (PAN) were monitored at the National Reference Climatological Station in Hangzhou before, during and after the G20 summit (August 15–September 24, 2016). The variations and sources of  $PM_{10}$ ,  $PM_{0.1}$  and  $PM_{0.01}$  in the location were investigated in depth. To the best of our knowledge, this is the first report to investigate the effect of radical emission reduction schemes on the size distribution of submicron aerosols.

## METHODS

The sampling site (120°10'E, 30°14'N) was located at the National Reference Climatological Station on a hill (altitude 42 m) near famous West Lake at Hangzhou. The station was run by Meteorological Bureau of Zhejiang Province to present typical urban background environment. The sampling period was from August 15 to September 24 in 2016. Excluding September 11–16 with sporadic rain events,

there are total 35 valid observation days in this campaign.

Particle size distributions in the range from 3 to 750 nm were obtained by integrating two scanning mobility particle spectrometers (SMPS) with a nano-SMPS (a TSI differential mobility analyzer DMA3085 and a condensation particle counter CPC3776; scanning range: 3–64 nm) and a long SMPS (TSI DMA3081 and CPC3775; scanning range: 64–750 nm). Scanning cycles of both SMPS systems were 4 min. The SMPSs sampled ambient air from a 129 cm long and 1.0 cm I.D. horizontally oriented SS tube with an airflow of 14 standard L min<sup>-1</sup>. The transport loss of particles in the SMPS inlets was corrected using size-dependent survival ratios of 85–100% for particles > 3 nm. Prior to the campaign, calibration of particle instruments was made using standard polystyrene latex particle (Yu *et al.*, 2016; Dai *et al.*, 2017).  $PM_{0.1}$  and  $PM_{0.01}$  in this study were calculated from the SMPS data by integrating particle mass from 3 nm to 100 nm and 3 nm to 10 nm, respectively, assuming all particles to be spherical with a density of 1.5 g cm<sup>-3</sup>.

Hourly gaseous PAN was analyzed using a modified Hewlett-Packard 7890B gas chromatograph equipped with a <sup>63</sup>Ni electron capture detector and a capillary column DB-1 (30 m length, 0.32 mm ID, 1.0 μm film thickness, Agilent Technologies). The detection limits (three times the signal to noise) of PAN was 22 pptv. The overall uncertainty for measuring atmospheric PAN was estimated to be ± 15% based on the combined uncertainties of the GC precision and the uncertainties of NO<sub>x</sub> calibration system. More detailed description of the instrument can be found in the paper of Zhang *et al.* (2012).

The concentrations of anions and cations (Cl<sup>-</sup>, SO<sub>4</sub><sup>2-</sup>, NO<sub>3</sub><sup>-</sup>, Na<sup>+</sup>, NH<sub>4</sub><sup>+</sup>, K<sup>+</sup>, Mg<sup>2+</sup>, and Ca<sup>2+</sup>) in  $PM_{10}$  were measured with a 60-min time resolution using the Ambient Ion Monitor-Ion Chromatograph (AIM-IC, URG Corp, Chapel Hill, NC, United States). The operation principle of AIM-IC is described in details by Markovic *et al.* (2012).  $PM_{10}$  mass concentration was measured with a tapered element oscillating microbalance (TEOM, Model 1400a; Rupprecht & Pataschnick Co., Inc., United States). The inlet for the AIM and TEOM was equipped with a 1-μm-diameter cutoff size cyclone (Model URG-2000-30EHB, URG Incorporated, United States). A total flow of 16.7 L min<sup>-1</sup> was drawn into the system. The flow was then split for the two instruments.

## RESULTS AND DISCUSSION

### Diurnal Variations of $PM_{10}$ , $PM_{0.1}$ and $PM_{0.01}$

Fig. 2 presents the mean diurnal variations of  $PM_{10}$ ,  $PM_{0.1}$

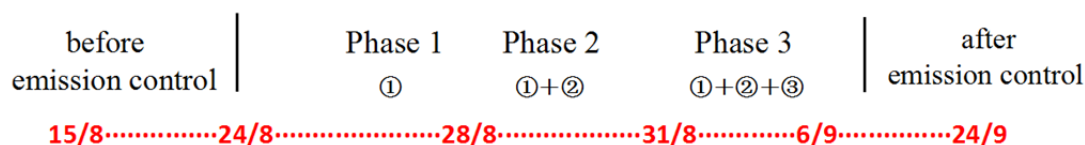


**Fig. 1.** The three-phase scheme during the emission control period for the 2016 G20 summit. Control strategies included ① coal-fired power plant capacity reduction of 50%, ② “odd-even” on-road vehicle restriction and ③ VOC emission reduction of 100% from industrial sectors (e.g., refinery and chemical processes/facilities).

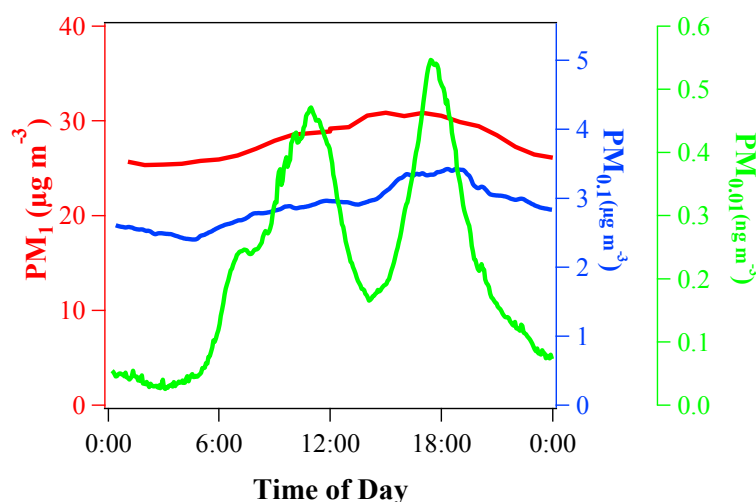


**Fig. 2.** Mean diurnal variation of  $PM_1$  (red line),  $PM_{0.1}$  (blue line) and  $PM_{0.01}$  (green line) during the observation period.

and  $PM_{0.01}$  during the observation period. It was found that the average mass concentration of  $PM_{0.1}$  was  $2.9 \pm 0.3 \mu\text{g m}^{-3}$ , accounting for  $10.3 \pm 0.5\%$  of  $PM_1$ .  $PM_1$  and  $PM_{0.1}$  showed a similar unimodal diurnal variation. Maximum concentration of  $PM_1$  was observed during 14:00–18:00 (local time). Maximum  $PM_{0.1}$  was recorded a few hours later around 16:00–19:00. Earlier studies reported that long-term  $PM_{2.5}$  observations in megacities like Beijing and New York City generally presented a bimodal pattern, showing a first peak around 7:00 attributed to enhanced traffic during morning rush hours and a second peak around 22:00 due to the decrease of boundary layer height (BLH) (Degaetano and Doherty, 2004; Liu *et al.*, 2015). The different patterns of  $PM_1$  from the reported  $PM_{2.5}$  indicated that  $PM_1$  in Hangzhou was dominated by daytime primary emission or secondary formation, rather than the evolution of boundary layer.

Different from  $PM_1$  and  $PM_{0.1}$ ,  $PM_{0.01}$  showed a trimodal diurnal variation on both NPF and non-NPF days (Fig. S1). Three peaks showed up at around 7:00, 11:00 and 18:00 with concentrations of  $0.25 \pm 0.18$ ,  $0.47 \pm 0.15$  and  $0.55 \pm 0.24 \text{ ng m}^{-3}$ , respectively, much higher than the average concentration of  $0.13 \pm 0.04 \text{ ng m}^{-3}$  during the nighttime (Fig. 2). The first peak showed up as a small shoulder of the second peak, but became more prominent on non-NPF days (see Section 3.2). Based on the occurrence time of the first and third peaks, it can be inferred that they were most likely associated with vehicle emissions during rush hours. The second peak was not affected by vehicle emission reduction but was enhanced during NPF events. This will be discussed in detail in Section 3.2.

#### **Impact of Emission Reductions on $PM_1$ , $PM_{0.1}$ and $PM_{0.01}$**

Fig. 3 shows particle mass size spectrum, 100–750 nm particle number concentration and  $PM_1$  mass concentration during the observation period. Ground-level wind speed and daily maximum boundary layer height (BLH) inverted from Micro Pulse LiDAR measurement (Sigma Space, Lanham, United States) were also presented.  $PM_1$  mass concentration was found to decrease during the coal-fired power plant emission control period from August 24 to

September 6. Excluding the two pollution episodes on September 3 and September 4, the mean mass concentration of  $PM_1$  during the control period was  $16 \pm 6.2 \mu\text{g m}^{-3}$ , which was 40% and 58% lower than the mean concentrations before and after the control period, respectively. In the meanwhile, we did not observe favorable meteorological conditions, such as higher wind speed and BLH, during the control period. HYSPLIT back trajectory analysis showed that before, during and after the control period, air masses all originated from East China Sea or coastal line of eastern China, except that stagnant air mass was coming westerly during the two episodes on September 3 and 4. Furthermore,  $PM_1$  reduction was not seen after the beginning of traffic and VOC emission controls (i.e., Phase 2 and 3). These evidences indicated that the decrease of  $PM_1$  mass concentration was mainly benefited from the coal-fired power plants emission reduction.

Particle mass concentration is determined by two factors: number concentration and particle size. Based on our measurement, 100–750 nm aerosols contributed more than 90% to the total mass concentration from 3 nm to 750 nm, assuming particle density to be constant for all particle sizes. The number concentration of 100–750 nm particles was  $4000 \pm 800 \text{ cm}^{-3}$  during the entire observation period and did not exhibit statistically lower concentrations throughout the control period. On the other hand, we fitted the measured mass size distributions with log-normal distribution functions in each SMPS time interval. The mode diameters of the log-normal distributions were shown on the size spectra in Fig. 3. It can be found that, except the two  $PM_1$  pollution episodes on September 3 and 4, the mode diameters of  $PM_1$  decreased significantly to  $253 \pm 40 \text{ nm}$  during the control period, which was 52 nm and 80 nm lower than those before and after the control period, respectively. It is thus apparent that the decrease of  $PM_1$  was mainly due to the decrease of particle sizes, rather than particle number concentrations. This implied that during the power plant emission control period the growth of ambient particles was slower with less contribution of secondary aerosols converted from gas phase.

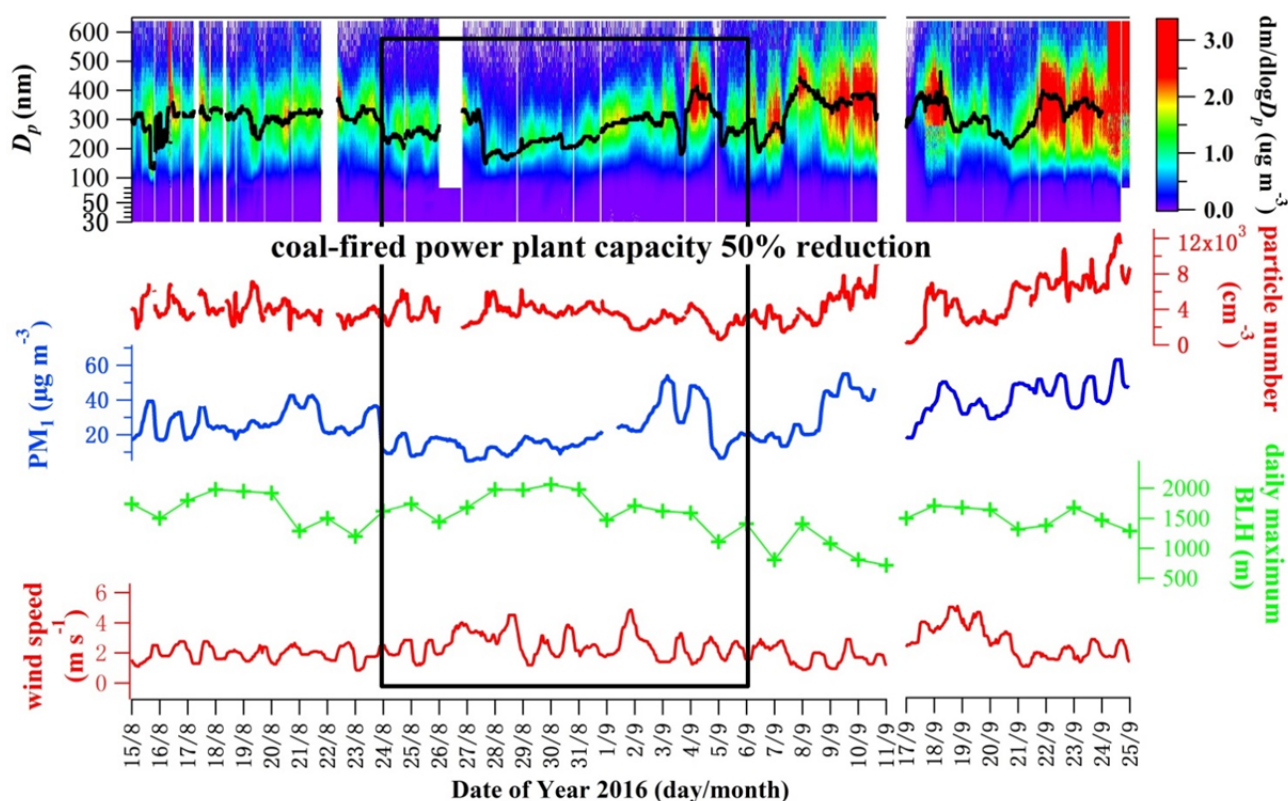


**Fig. 3.** from upper to lower: mass spectra and mode diameter (black line), 100–750 nm particle number concentration (red line),  $PM_{10}$  mass concentration (blue line) of atmospheric aerosols, ground level wind speed and daily maximum boundary layer height (BLH) during the observation period. The black box highlights the power plant emission control period during G20.

Fig. 4 shows  $PM_{0.1}$  mass concentration, PAN and particle number size spectra throughout the observation period. Although  $PM_{0.1}$  mass concentration accounted for  $10.3 \pm 3.5\%$  in  $PM_{10}$ ,  $PM_{0.1}$  contributed  $83 \pm 15\%$  and  $54 \pm 20\%$  to  $PM_{10}$  in terms of number concentration in the daytime and nighttime, respectively. The coal-fired power plants capacity reduction since August 24 and “odd-even” on-road vehicle restriction since August 28 seemed to have no obvious effect on  $PM_{0.1}$  concentration before the enforcement of VOC emission control. Whilst during August 31–September 6 (VOC emission control),  $PM_{0.1}$  mass concentration and PAN decreased significantly by 53% and 55% to  $1.3 \pm 0.6 \mu\text{g m}^{-3}$  and  $1.0 \pm 0.7 \text{ ppbv}$ , respectively. Furthermore, the correlation coefficient  $R$  between PAN and  $PM_{0.1}$  was 0.85. Considering the shorter lifetime of PAN in the nighttime than  $PM_{0.1}$  due to rapid PAN thermal decomposition (Roberts *et al.*, 1998), this correlation is deemed strong. PAN is a secondary product in the photochemical reactions of nitrogen oxides and volatile organic compounds (Zhang *et al.*, 2015; Liu *et al.*, 2010) and is regarded as an indicator of atmospheric photochemical pollution (Fischer *et al.*, 2014). Therefore, the high correlation indicated that  $PM_{0.1}$ , or at least the majority of  $PM_{0.1}$ , and PAN shared a common atmospheric oxidation formation pathway from VOCs.

Previous source apportionment studies of Shen *et al.* (2014) and Wu *et al.* (2014) have found that vehicle emission is the most important contributor to  $PM_{10}$  in Hangzhou.

However, no evident reduction of  $PM_{10}$  was observed in this study by comparing before and after the implementation of “odd-even” on-road vehicle restriction. The difference of  $PM_{0.1}$  was also not seen before or after the vehicle restriction. Instead, it can be seen in Fig. 5(a) that sub-10 nm nanoparticle concentrations in rush hours around 07:00 and 18:00 decreased dramatically by 48% and 42% after the enforcement of “odd-even” on-road vehicle restriction, as compared to that before the enforcement. The second  $PM_{0.01}$  peak at around 11:00, however, decreased to a lesser degree by 16%. The source of sub-10 nm particles was further explored by comparing  $PM_{0.01}$  on NPF days and non-NPF days. An NPF day was defined as a day with a banana-shaped particle growth curve starting from 3 nm to more than 60 nm on the particle number size spectra (Dal Maso *et al.*, 2007; Yu *et al.*, 2014a, b).  $PM_{0.01}$  diurnal variations in Fig. 5(b) showed that the second  $PM_{0.01}$  peak was enhanced on the NPF days by a factor of 4 compared to that of the non-NPF days. Again, the enhancement of  $PM_{10}$  and  $PM_{0.1}$  by NPF was not seen and thus not shown here. The evidences above indicated that the vehicle emission and the regional NPF events were the two sources of nanoparticles below 10 nm in the urban atmosphere of Hangzhou.

Based on Fig. 3, during the 7 days right before the enforcement of VOC emission reduction, the emission control schemes implemented during Phase 1 and 2 had not suppressed NPF occurrence completely, as there were



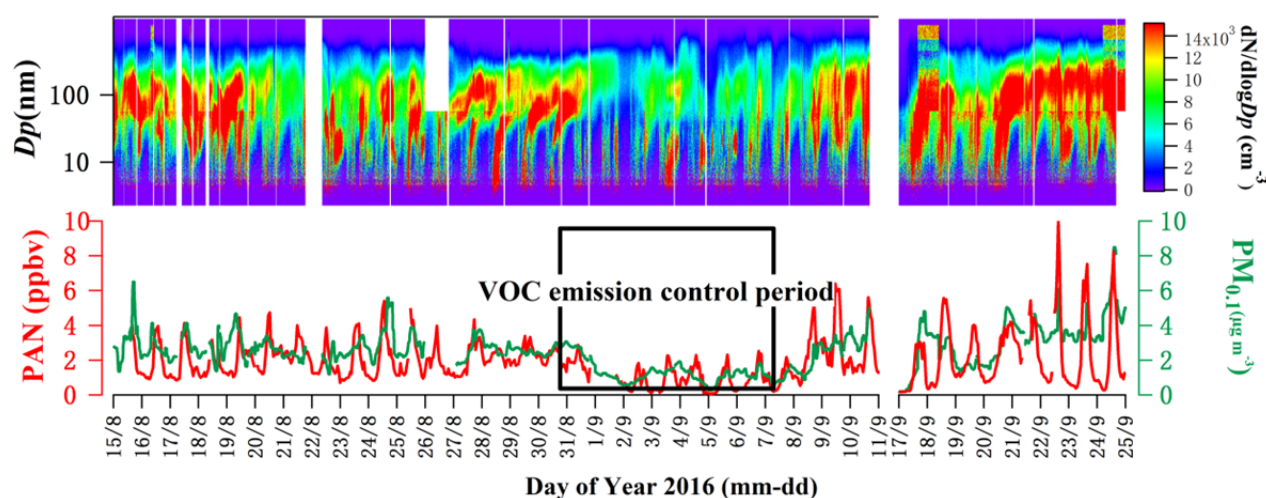


**Fig. 4.** Upper: particle number size spectra during the observation period. Lower: mass concentration of  $PM_{0.1}$  (green line) and PAN (red line) during the observation period. The black box highlights the VOC emission control period.

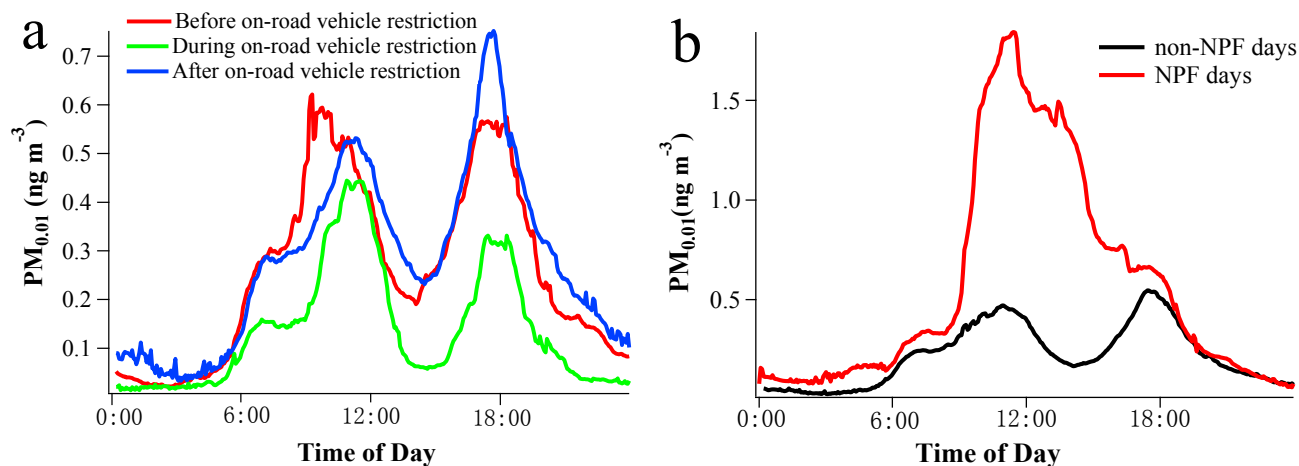


**Fig. 5.** Mean diurnal variations of  $PM_{0.01}$  (a) before (red line), during (green line) and after (blue line) the “odd-even” on-road vehicle restriction and (b) on NPF days (red line) and non-NPF days (black line).

4 typical NPF events on August 25, 27, 28 and 29. It is possible that  $PM_1$ , as a surrogate of condensation sink/coagulation sink for nucleation precursors and clusters, were reduced in the Phase 1 and 2 periods. On the other hand, the supply of VOCs, as nucleation precursors, was still high in these two phases. As a result, high VOCs precursor and low condensation/coagulation sink facilitate the NPF occurrence. Noticeably, the NPF events after the emission control period occurred every day from September 17 to 23. The high  $PM_1$  (Fig. 3) and PAN concentrations (Fig. 4) during this period suggested that both nucleation precursor and condensation/coagulation sink were high. The NPF in such highly polluted condition can be explained that strong low-volatile vapor supply out-competed strong condensation/coagulation scavenging by pre-existing particles (Yu *et al.*, 2017, and references therein).

#### Two $PM_1$ Episodes during the Phase 3 Control Period

Although the strictest emission control scheme was enforced during the Phase 3 period from August 31 to

September 6, two  $PM_1$  episodes were still observed on September 3 and September 4 (Fig. 3). Maximum  $PM_1$  concentrations reached up to  $51.9 \mu g m^{-3}$  and  $48.1 \mu g m^{-3}$  in the two episodes respectively, which increased by 146% and 128% than the average level of the rest of days during the Phase 3 period. In addition, particle mode diameters reached up to 316 nm and 399 nm in the two episodes, while it was only  $253 \pm 39.2$  nm during the rest of days during the Phase 3 period.

Fig. 6 shows the mass concentrations of  $PM_1$  and water-soluble inorganic ions of  $SO_4^{2-}$ ,  $NO_3^-$ ,  $NH_4^+$  and  $K^+$  during the emission control period. When  $PM_1$  reached the maximum concentration in Episode 1, the sum of secondary inorganic ions ( $SO_4^{2-}$ ,  $NO_3^-$  and  $NH_4^+$ : SNA) increased by ~100% as compared to that on the rest of days in Phase 3. The boost of SNA accounted for 47% of the total increment in  $PM_1$ . In Episode 2, the concentration of SNA increased by 152% and accounted for 62.5% of the total increment of  $PM_1$ . The concentration of nss- $K^+$ , as a tracer of biomass burning aerosol (Khalil and Rasmussen, 2003), increased

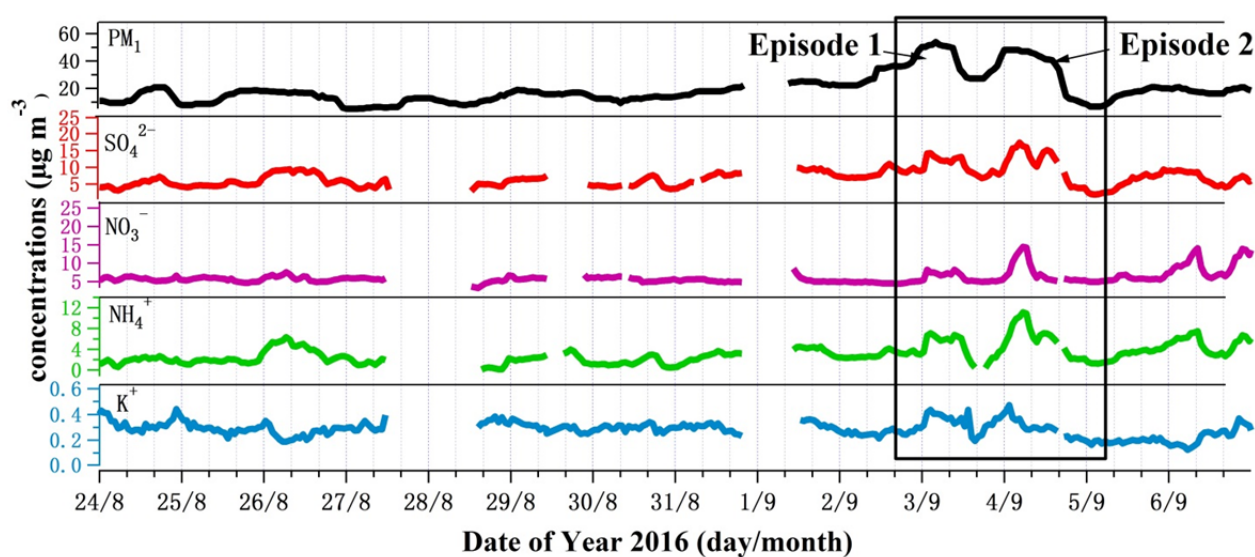


**Fig. 6.** Mass concentrations of PM<sub>1</sub> (black line) and water-soluble inorganic ions (SO<sub>4</sub><sup>2-</sup>, red line; NO<sub>3</sub><sup>-</sup>, purple line; NH<sub>4</sub><sup>+</sup>, green line; K<sup>+</sup>, blue line) during the emission control period. The black box shows the two PM episodes on September 3, 2016 (episode 1) and September 4 2016 (episode 2).

by 21% and 23% in Episodes 1 and 2, respectively. It indicated that secondary inorganics and biomass burning emission were important contributors in the two episodes.

To investigate the source of the two episodes, the Weather Research and Forecast Model with Chemistry (WRF-Chem) was used to simulate the daily variation of PM<sub>1</sub> at the studied site from September 2 to 7, 2016. The details of model setup can be found in Supporting Information. Two scenarios were tested in this study. In Scenario A, an anthropogenic emission inventory was made based on the Multi-resolution Emission Inventory for China (MEIC) for the year 2012 (Lei *et al.*, 2011) and the radical emission reduction scheme implemented in the emission control region during the Phase 3 period. In Scenario B, all anthropogenic and biogenic emissions were shut down in the emission control region.

The model results in Fig. 7(a) showed that the simulated PM<sub>1</sub> in Scenario A agreed well with the measured PM<sub>1</sub> with correlation coefficient  $R^2 = 0.64$ . The normalized mean bias was -26%. Importantly, the two PM<sub>1</sub> episodes on September 3 and 4 could be reproduced by the model simulation Scenario A. By comparing the results between Scenario A and B, the contributions to PM<sub>1</sub> from the sources inside and outside the region of emission control can be acquired. The result showed that the contribution from the sources inside the emission control region ranged from 70% to 83% during the simulation period excluding the pollution episodes. The contributions increased to 94% and 85% in Episode 1 and 2, respectively, while the remaining 6% and 15% were from the transport of aerosols from outside the region. The simulation thus suggested that PM<sub>1</sub> in Hangzhou from September 2 to 7 was mainly from the sources inside the emission control region and the effective PM<sub>1</sub> concentration reduction during this period can be convincingly attributed to the emission control measures enforced inside the region.

The above simulation also suggested that the two PM<sub>1</sub> episodes were not the consequence of long-range transport of pollutants from outside into the emission control region. The model simulation showed that isobars in this region were spaced far apart and ground-level wind speed was low during the two episodes. In Fig. 7(b), the vertical cross section of temperature and wind profiles in Episode 1, for example, showed that the temperature gradient was weak and the atmosphere was dominated by subsidence flows up to 600 meters above ground in Hangzhou. High concentration of PM<sub>1</sub> was seen above Hangzhou and also the region to the east of Hangzhou (Fig. 7(b)). Therefore, the episodes were very likely the consequence of the synoptic weather conditions that were favorable for the accumulation of submicron aerosols.

## CONCLUSIONS

The short-term reduction of source emissions from coal-fired power plants, on-road vehicles and industrial VOCs during the G20 summit provides a unique opportunity to gain insight into the sources of submicron aerosols in Hangzhou, a megacity in eastern China. We conducted particle size distribution measurements to investigate the effect of the three-phase control scheme on PM<sub>1</sub>, PM<sub>0.1</sub> and PM<sub>0.01</sub> at an urban background site in Hangzhou. The WRF-Chem simulation suggested that the sources inside the emission control region contributed more than 70% to PM<sub>1</sub> from September 2 to 7, 2016, in Hangzhou, even under the strictest control scheme. The 50% reduction of the coal-fired power plant capacity suppressed the growth of particles and decreased PM<sub>1</sub> by 40% and 58% compared to before and after the control period. Sub-10 nm nanoparticle concentrations declined by 48% and 42% in the morning and evening rush hours, respectively, after the implementation of a 50% reduction of on-road vehicles.

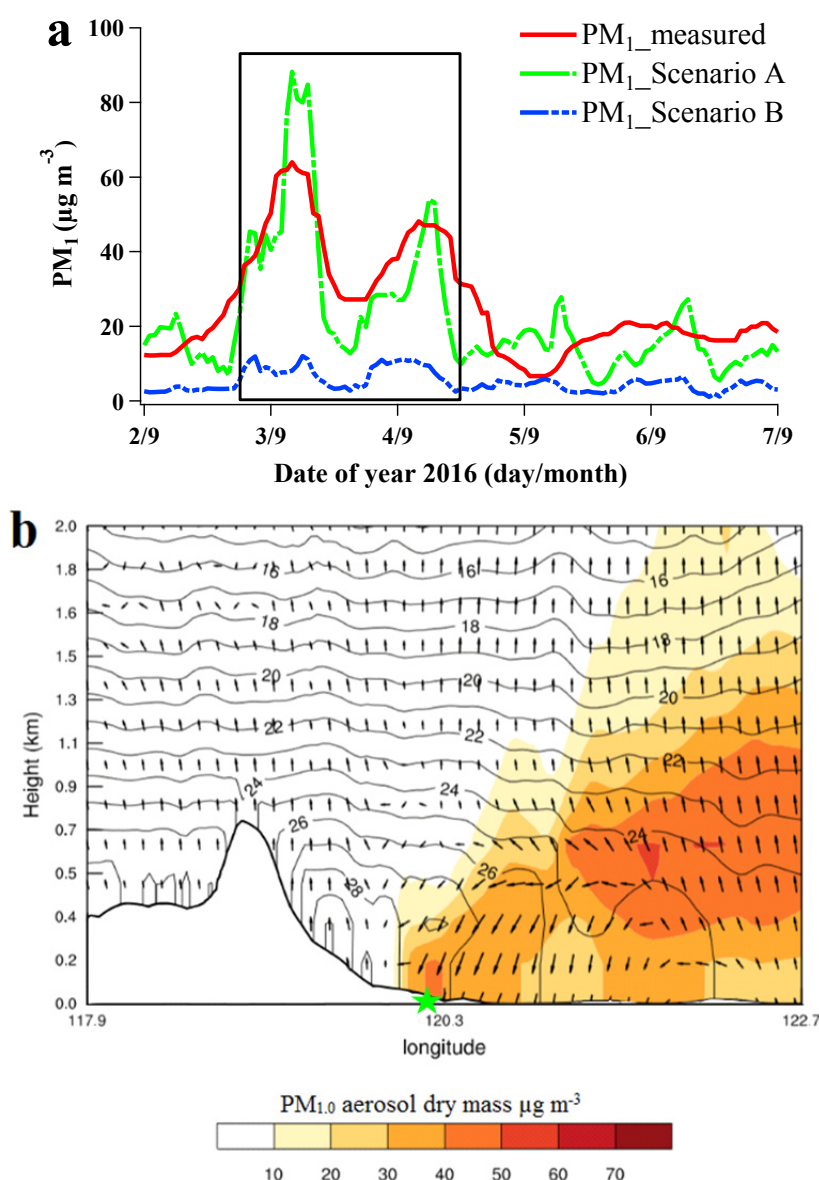


**Fig. 7.** (a) Simulated and measured PM<sub>1</sub> concentrations from September 2–7, 2016. (b) Vertical cross section of temperature, wind and PM<sub>1</sub> dry mass concentration profiles from west to east at local time 00:00 on September 3, 2016. The solid line in the left corner indicates the terrain surface. The green star indicates the location of Hangzhou.

The 100% reduction of VOC emissions from industrial sectors enforced during the Phase 3 period resulted in a 53% decrease in the PM<sub>0.1</sub> concentration.

The emission control did not completely suppress the occurrence of NPF. Four typical NPF events occurred out of 7 days in Phase 1 and Phase 2, probably due to a low condensation/coagulation sink, differing from NPF events after the emission control period, when both the nucleation precursor and coagulation sink were high. The NPF events were found to be an important source of nanoparticles smaller than 10 nm. The PM<sub>0.01</sub> peak concentration around 11:00 AM was enhanced on NPF days by a factor of 4 compared to non-NPF days.

Although the strictest emission control scheme was enforced during the Phase 3 period from August 31 to September 6, two PM<sub>1</sub> episodes were still observed. The

model simulation suggested that the two episodes did not result from the intrusion of pollutants from outside the emission control region. Instead, the episodes were due to the unfavorable synoptic situations, including the dominance of subsidence airflows, a weak wind and a weak vertical temperature gradient. Larger particle sizes and enhanced secondary inorganic content were detected in PM<sub>1</sub> during the two episodes.

#### ACKNOWLEDGMENTS

The authors would like to thank the National Key Research and Development Program of China (2016YFC0203100), the National Science Foundation of China (grant numbers 41675124 and 91544229) and Jiangsu Specially Appointed Professor Grant.

## SUPPLEMENTARY MATERIAL

Supplementary data associated with this article can be found in the online version at <http://www.aaqr.org>.

## REFERENCES

- Aurela, M., Saarikoski, S., Niemi, J.V., Canonaco, F., Prevot, A.S.H., Frey, A., Carbone, S., Kousa, A. and Hillamo, R. (2015). Chemical and Source characterization of submicron particles at residential and traffic sites in the Helsinki metropolitan area, Finland. *Aerosol Air Qual. Res.* 15: 1213–1226.
- Carbone, S., Saarikoski, S., Frey, A., Reyes, F., Reyes, P., Castillo, M., Gramsch, E., Oyola, P., Jayne, J., Worsnop, D.R. and Hillamo, R. (2013). Chemical characterization of submicron aerosol particles in Santiago de Chile. *Aerosol Air Qual. Res.* 13: 462–473.
- Dai, L., Wang, H., Zhou, L., An, J., Tang, L., Lu, C., Yan, W., Liu, R., Kong, S. and Chen, M. (2017). Regional and local new particle formation events observed in the Yangtze River Delta region, China. *J. Geophys. Res. Atmos.* 122: 2389–2402.
- Dal Maso, M., Sogacheva, L., Aalto, P.P., Riipinen, I., Komppula, M., Tunved, P., Korhonen, L., Suur-Uski, V., Hirsikko, A., Kurtén, T., Kerminen, V.M., Lihavainen, H., Viisanen, Y., Hansson, H.C. and Kulmala, M. (2007). Aerosol size distribution measurements at four Nordic field stations: identification, analysis and trajectory analysis of new particle formation bursts. *Tellus B* 59: 350–361.
- Degaetano, A.T. and Doherty O.M. (2004). Temporal, spatial and meteorological variations in hourly PM<sub>2.5</sub> concentration extremes in New York City. *Atmos. Environ.* 38: 1547–1558.
- Fischer, E.V., Jacob, D.J., Yantosca, R.M., Sulprizio, M.P., Millet, D.B., Mao, J., Paulot, F., Singh, H.B., Roiger, A. and Ries, L. (2014). Atmospheric peroxyacetyl nitrate (PAN): A global budget and source attribution. *Atmos. Chem. Phys.* 14: 2679–2698.
- Gaston, C.J., Riedel, T.P., Zhang, Z., Gold, A., Surratt, J.D. and Thornton, J.A. (2014). Reactive uptake of an isoprene-derived epoxydiol to submicron aerosol particles. *Environ. Sci. Technol.* 48: 11178–11186.
- Guo, J., He, J., Liu, H., Miao, Y., Liu, H. and Zhai, P. (2016). Impact of various emission control schemes on air quality using WRF-Chem during APEC China 2014. *Atmos. Environ.* 14: 311–319.
- Guo, S., Hu, M., Zamora, M.L., Peng, J., Shang, D., Zheng, J., Du, Z., Wu, Z., Shao, M., Zeng, L., Molina, M.J. and Zhang, R. (2014). Elucidating severe urban haze formation in China. *Proc. Natl. Acad. Sci. U.S.A.* 111: 17373–17378.
- Hu S.W., Wu, X.F., Luo K., Gao, X. and Fan, J.R. (2015). Source apportionment of air pollution in Hangzhou city based on CMAQ. *Energy Eng.* 7: 40–44.
- Hua, Y., Wang, S., Wang, J., Jiang, J., Zhang, T., Song, Y., Kang, L., Zhou, W., Cai, R., Wu, D., Fan, S., Wang, T., Tang, X., Wei, Q., Sun, F. and Xiao, Z. (2016). Investigating the impact of regional transport on PM<sub>2.5</sub> formation using vertical observation during APEC 2014 Summit in Beijing. *Atmos. Chem. Phys.* 16: 15451–15460.
- Huang, K., Zhuang, G., Lin, Y. and Wang, Q. (2013). How to improve the air quality over mega-cities in China? – Pollution characterization and source analysis in Shanghai before, during, and after the 2010 World Expo. *Atmos. Chem. Phys.* 13: 5927–5942.
- IPCC (2013). *Climate Change 2013: The Physical Science Basis, Contribution of Working Group I to the Fifth Assessment Report to the Intergovernmental Panel on Climate Change*. Cambridge University Press, Cambridge, United Kingdom and New York, NY, USA, 2013.
- Khalil, M.A.K. and Rasmussen, R.A. (2003). Tracers of wood smoke. *Atmos. Environ.* 37: 1211–1222.
- Kim, H., Kim, J.Y., Kim, J.S. and Jin, H.C. (2015). Physicochemical and optical properties of combustion-generated particles from a coal-fired power plant, automobiles, ship engines, and charcoal kilns. *Fuel* 161: 120–128.
- Kulmala, M., Kerminen, V.M., Petaja, T., Ding, A. and Wang, L. (2017). Atmospheric gas-to-particle conversion: Why NPF events are observed in megacities? *Faraday Discuss.* 200: 271–288.
- Lei, Y., Zhang, Q., He, K.B. and Streets, D.G. (2011). Primary anthropogenic aerosol emission trends for China, 1990–2005. *Atmos. Chem. Phys.* 11: 17153–17212.
- Li, P., Wang, L., Guo, P., Yu, S., Mehmood, K., Wang, S., Liu, W., Seinfeld, J.H., Zhang, Y., Wong, D.C., Alapaty, K., Pleim, J. and Mathur, R. (2017). High reduction of ozone and particulate matter during the 2016 G-20 summit in Hangzhou by forced emission controls of industry and traffic. *Environ. Chem. Lett.* 15: 709–715.
- Liu, Z., Wang, Y., Gu, D., Zhao, C., Huey, L.G., Stickel, R., Liao, J., Shao, M., Zhu, T. and Zeng, L. (2010). Evidence of reactive aromatics as a major source of peroxy acetyl nitrate over China. *Environ. Sci. Technol.* 44: 7017–7022.
- Liu, Z., Hu, B., Wang, L., Wu, F., Gao, W. and Wang, Y. (2015). Seasonal and diurnal variation in particulate matter (PM<sub>10</sub> and PM<sub>2.5</sub>) at an urban site of Beijing: Analyses from a 9-year study. *Environ. Sci. Pollut. Res. Int.* 22: 627–642.
- Markovic, M.Z., Vandenboer, T.C. and Murphy, J.G. (2012). Characterization and optimization of an online system for the simultaneous measurement of atmospheric water-soluble constituents in the gas and particle phases. *J. Environ. Monit.* 14: 1872–1884.
- Meng, R., Zhao, F., Sun, K., Zhang, R., Huang, C. and Yang, J. (2015). Analysis of the 2014 “APEC Blue” in Beijing using more than one decade of satellite observations: Lessons learned from radical emission control measures. *Remote Sens.* 7: 15224.
- Ostro, B., Hu, J., Goldberg, D., Reynolds, P., Hertz, A., Bernstein, L. and Kleeman, M. J. (2015). Associations of Mortality with Long Term Exposures to Fine and Ultrafine Particles, Species and Sources: Results from the California Teachers Study Cohort. *Environ. Health*



- Perspect.* 123: 549–556.
- Pui, D.Y.H., Chen, S.C. and Zuo, Z. (2014). PM<sub>2.5</sub> in China: Measurements, sources, visibility and health effects, and mitigation. *Particuology* 13: 1–26.
- Roberts, J.M., Williams, J., Baumann, K., Buhr, M.P., Goldan, P.D., Holloway, J., Hübler, G., Kuster, W.C., McKeen, S.A., Ryerson, T.B., Trainer, M., Williams, E.J., Fehsenfeld, F.C., Bertman, S.B., Nouaime, G., Seaver, C., Grodzinsky, G., Rodgers, M. and Young, V.L. (1998). Measurements of PAN, PPN, and MPAN made during the 1994 and 1995 Nashville Intensives of the Southern Oxidant Study: Implications for regional ozone production from biogenic hydrocarbons. *J. Geophys. Res.* 103: 22473–22490.
- Shen, J., Jiao, L., Chang, X.U., Xi, H.E., Ying, F. and Hong, S. (2014). Source apportionment of size-resolved ambient fine particulate matter in Hangzhou. *J. Univ. Chin. Acad. Sci.* 31: 367–373.
- Shen, Z., Cao, J., Tong, Z., Liu, S., Reddy, L.S.S., Han, Y., Zhang, T. and Zhou, J. (2009). Chemical characteristics of submicron particles in winter in Xi'an. *Aerosol Air Qual. Res.* 9: 80–93.
- Shi, J.P., Evans, D.E., Khan, A.A. and Harrison, R.M. (2001). Sources and concentration of nanoparticles. *Atmos. Environ.* 35: 1193–1202.
- Singh, D.K. and Gupta, T. (2016). Effect through inhalation on human health of PM<sub>1</sub> bound polycyclic aromatic hydrocarbons collected from foggy days in northern part of India. *J. Hazard. Mater.* 306: 257–268.
- Sun, Y.L., Zhang, Q., Zheng, M., Ding, X., Edgerton, E.S. and Wang, W.X. (2011). Characterization and source apportionment of water-soluble organic matter in atmospheric fine particles (PM<sub>2.5</sub>) with high-resolution aerosol mass spectrometry and GC-MS. *Environ. Sci. Technol.* 45: 4854–4861.
- Wang, G., Cheng, S., Lang, J., Yang, X., Wang, X., Chen, G., Liu, X. and Zhang, H. (2017). Characteristics of PM<sub>2.5</sub> and assessing effects of emission reduction measures in the heavy polluted city of Shijiazhuang, before, during, and after the Ceremonial Parade 2015. *Aerosol Air Qual. Res.* 17: 499–512.
- Wang, S., Zhao, M., Xing, J., Wu, Y., Zhou, Y., Lei, Y., He, K., Fu, L. and Hao, J. (2010). Quantifying the air pollutants emission reduction during the 2008 Olympic Games in Beijing. *Environ. Sci. Technol.* 44: 2490–2496.
- Wu, L., Shen, J.D., Feng, Y.C., Bi, X.H., Jiao, L. and Liu, S.X. (2014). Source apportionment of particulate matters in different size bins during hazy and non-hazy episodes in Hangzhou City. *Res. Environ. Sci.* 27: 373–381.
- Yang, X., Cheng, S., Li, J., Lang, J. and Wang, G. (2017). Characterization of chemical composition in PM<sub>2.5</sub> in Beijing before, during, and after a large-scale international event. *Aerosol Air Qual. Res.* 17: 896–907.
- Yu, H., Gannet Hallar, A., You, Y., Sedlacek, A., Springston, S., Kanawade, V.P., Lee, Y.N., Wang, J., Kuang, C., McGraw, R.L., McCubbin, I., Mikkilä, J. and Lee, S.H. (2014a). Sub-3 nm particles observed at the coastal and continental sites in the United States. *J. Geophys. Res.* 119: 860–879.
- Yu, H., Ortega, J., Smith, J.N., Guenther, A.B., Kanawade, V.P., You, Y., Liu, Y., Hosman, K., Karl, T., Seco, R., Geron, C., Pallardy, S.G., Gu, L., Mikkilä, J. and Lee, S.H. (2014b). New particle formation and growth in an isoprene-dominated Ozark forest: From sub-5 nm to CCN-Active sizes. *Aerosol Sci. Technol.* 48: 1285–1298.
- Yu, H., Zhou, L., Dai, L., Shen, W., Dai, W., Zheng, J., Ma, Y. and Chen, M. (2016). Nucleation and growth of sub-3 nm particles in the polluted urban atmosphere of a megacity in China. *Atmos. Chem. Phys.* 16: 18653–18690.
- Yu, H., Ren, L. and Kanawade, V. P. (2017). New particle formation and growth mechanisms in highly polluted environments. *Curr. Pollution. Rep.* 3: 245–253.
- Yu, S., Zhang, Q., Yan, R., Wang, S., Li, P., Chen, B., Liu, W. and Zhang, X. (2014). Origin of air pollution during a weekly heavy haze episode in Hangzhou, China. *Environ. Chem. Lett.* 12: 543–550.
- Zhang, G., Mu, Y., Liu, J. and Mellouki, A. (2012). Direct and simultaneous determination of trace-level carbon tetrachloride, peroxyacetyl nitrate, and peroxypropionyl nitrate using gas chromatography-electron capture detection. *J. Chromatogr. A* 1266: 110–115.
- Zhang, G., Mu, Y., Zhou, L., Zhang, C., Zhang, Y., Liu, J., Fang, S. and Yao, B. (2015). Summertime distributions of peroxyacetyl nitrate (PAN) and peroxypropionyl nitrate (PPN) in Beijing: Understanding the sources and major sink of PAN. *Atmos. Environ.* 103: 289–296.
- Zhang, Y., Tang, L., Croteau, P.L., Favez, O., Sun, Y., Canagaratna, M.R., Wang, Z., Couvidat, F., Albinet, A., Zhang, H., Sciare, J., Prévôt, A.S.H., Jayne, J.T. and Worsnop, D.R. (2017). Field characterization of the PM<sub>2.5</sub> Aerosol Chemical Speciation Monitor: insights into the composition, sources, and processes of fine particles in eastern China. *Atmos. Chem. Phys.* 17: 14501–14517.
- Zhou, D., Li, B., Huang, X., Virkkula, A., Wu, H., Zhao, Q., Zhang, J., Liu, Q., Li, L., Li, C., Chen, F., Yuan, S., Qiao, Y., Shen, G. and Ding, A. (2017). The impacts of emission control and regional transport on PM<sub>2.5</sub> ions and carbon components in Nanjing during the 2014 Nanjing Youth Olympic Games. *Aerosol Air Qual. Res.* 17: 730–740.

Received for review, February 22, 2017

Revised, May 18, 2018

Accepted, June 8, 2018